SPACE TELESCOPE SCIENCE INSTITUTE
Operated for NASA by AURA

COS Instrument Science Report 2010-06(v1)

SMOV: COS FUV Wavelength Calibration

Cristina Oliveira, Stéphane Béland, Charles (Tony) Keyes, & Sami Niemi
February 19, 2010

ABSTRACT

COS calibration program 11487 was carried out during SMOV to characterize the wavelength scales of the FUV detector. Science data were obtained with the G130M, G160M, and G140L gratings through the Primary Science Aperture (PSA), simultaneously with PtNe lamp line spectra, obtained through the Wavelength Calibration Aperture (WCA). These data were partially calibrated with the COS pipeline and then, in conjunction with STIS data of the same target, used to derive offsets between the PSA and WCA wavelength scales. These offsets are then used to place the dispersion relations derived from thermal vacuum 2003 (TV03) in the on-orbit frame of reference, so that correct wavelengths can be assigned to the on-orbit COS data.

Contents:

1. Introduction

The COS FUV channel contains one low resolution (G140L) and two medium resolution (G130M, G160M) gratings, providing wavelength coverage from the Lyman limit to ∼2250 Å. Spectra of external targets are obtained through the Primary Science Aperture (PSA) while wavelength calibration spectra are obtained through the Wavelength Calibration Aperture (WCA). There are two PtNe line lamps on-board, and wavecal data can be obtained concurrently with science data (TAGFLASH mode) or either before or after a science exposure is obtained. Wavecal data is used by the COS pipeline (CalCOS) to correct for any offsets between the wavecals and the lamp template reference files due to non-repeatability of the grating mechanism positions. These offsets are then applied to the science data as well, before wavelengths are assigned (COS Data Handbook, Shaw et al. 2009).

During thermal vacuum 2003 (TV03) science (PSA) and wavecal (WCA) data were obtained at all central wavelengths of the FUV gratings, using an internal and an external PtNe line lamp. These data were used to derive dispersion relations for all the FUV modes (for FP-POS =3 only), by cross-correlating the observed spectra, in pixel space, with a PtNe wavelength line list. A linear dispersion relation was used for the medium resolution gratings (G130M and G160M) and a second order polynomial was used with the low dispersion grating (G140L). Because of the different optical paths between the PSA and WCA, the dispersion relations derived for each aperture are different. The dispersion solutions for the PSA are not adequately represented by a simple offset of the WCA dispersion solutions. A separate dispersion solution is needed per segment, for each central wavelength of each grating, for each aperture. Because the WCA and PSA have different dispersion solutions we cannot use WCA data obtained on-orbit to determine directly the on-orbit dispersion solutions for the PSA. Instead we use the PSA dispersion solutions derived from TV03 data to wavelength calibrate PSA data obtained on-orbit. However, the TV03 dispersion solutions cannot be directly applied to on-orbit data without placing the TV03 dispersion solutions on the on-orbit frame of reference, which implies deriving the on-orbit offsets between the PSA and WCA spectra, as described below. Note that all the FUV data needs to be thermally and geometrically corrected, assuring that the spectra are all in the same reference frame, before any other analysis.

Program 11487 was executed during SMOV to obtain spectra of external targets, that would allow us to determine the on-orbit offsets between the PSA and WCA data. These offsets are then used to place the dispersion relations derived in TV03 in the on-orbit frame of reference, so that correct wavelengths can be assigned to the on-orbit COS data, using the TV03-derived dispersion coefficients. As a first approximation we determine an average value, constant in wavelength for each setting, for the offsets between the PSA and WCA apertures. Future refinements to the FUV wavelength calibration will take into account the second order effect resulting from the fact that the PSA and WCA dispersion solutions are different, and so the offsets between the PSA and WCA are wavelength dependent.

Program 11488, a companion program to program 11487, was executed during SMOV with the purpose of obtaining wavelength calibration spectra through the WCA at all FP-POS, for all the central wavelengths of the FUV gratings, so that the lamp template reference file can be updated to the on-orbit frame of reference.

2. Observations

Data for the wavelength calibration of the FUV detector were obtained in program 11487 (COS FUV Internal/External Wavelength Scales). Table 1 summarizes the exposures taken in the different visits of this program. All the visits used a NUV target acquisition sequence consisting of ACQ/SEARCH (SCAN-SIZE=4; STEP-SIZE=1.767), followed by ACQ/SEARCH (SCAN-SIZE=2; STEP-SIZE=1.767), ACQ/PEAKXD, and ACQ/PEAKD (NUM-POS=9; STEP-SIZE=1.0) to achieve maximum centering accuracy. The optical element used for target acquisition is the first one given in Table 1, for each visit. All the exposures weere obtained in TIME-TAG mode and used special lamp flash parameters (available in ENG mode only) to ensure that multiple lamp flashes were present in each exposure (particularly for the longer exposures) and that any mechanism drift, if at all present, could be easily corrected.

Visit 01, observed NGC 6833 a compact planetary nebula that is slightly extended (0.2 arcsec) and for which the radial velocity is well known (-108.8 km/s). Visits 50 and 73 observed NGC 330–B37, a B super-giant in the SMC, which has been observed with STIS/E140M.

As part of the updating of the FUV wavelength scales, lamp template data was also obtained. Both the FUV and NUV lamp template reference files contain lamp spectra for each FP-POS, for each setting, which are used by CalCOS to calibrate data obtained at the corresponding FP-POS. Program 11488 (COS Internal FUV Wavelength Verification) obtained internal wavelength calibration spectra using the default PtNe lamp (Lamp 1) with each FUV grating, at each central wavelength setting, and for each FP-POS position. Each exposure had a duration of 120 sec. In order to allow the mechanism drift to settle after a grating motion, a 1800 sec exposure (containing multiple flashes of the lamp) was taken at the beginning of each visit. Analysis and results of the mechanism drift monitoring exposures will be presented in another ISR.

3. Data Analysis

To assess the impact of mechanism drift in the wavecal exposures obtained in program 11488 (this program obtains exposures that are used to update the lamp template referene file), each exposure was divided in 30 sec time slices, for each segment, and each time slice was cross-correlated with the first time slice. The maximum drift for any wavecal exposure was 1.3 pixels, but most were within 0.5 pixels, much smaller than the resolution element of 6 pixels, and so no drift correction was applied to the wavecal exposures.

After being corrected for thermal and geometric distortions, the wavecal data were extracted into 1d spectra (counts vs pixel) and then the 1d spectra were used to produce a new FUV lamp template reference file, containing one entry per FP-POS for each grating/cenwave/segment combination. In addition, each of the 1d spectra corresponding to FP-POS = 3 was cross-correlated with the 1d spectra for the same grating/cenwave/segment mode and FP-POS = 3 in the TV03-based lamp template reference file, in order to determine their separation, $\mathrm{WCA_{TV03}}$ - $\mathrm{WCA_{SMOV}}$. This value is needed so that the wavelength calibration is performed properly, as all the wavecal data obtained on-orbit is compared with a lamp template reference file that was also updated from on-orbit data. In addition, since the dispersion solutions from TV03, which are applied to the on-orbit data, and the lamp template reference file for TV03 are only for the FP-POS = 3 position the separation between the $\mathrm{WCA_{TV03}}$ - $\mathrm{WCA_{SMOV}}$ for other FP-POS is not necessary (see below).

3.1 NGC 330–B37

The rawtag files for each of the science exposures obtained in Visits 50 and 73 of program 11487 were partially calibrated with CalCOS by setting all the calibration switches to *OMIT* except for *TEMPCORR*, *GEOCORR*, *IGEOCORR*, *DOPPCORR*, and *WAVECORR*, which were set to *PERFORM*. The new lamp template reference file, described above, was used in this calibration, so that the exposures are placed in the on-orbit frame of reference. To produce 1d science and wavecal spectra, the *xfull* and *yfull* columns of the resulting corrtag files, which are corrected for temperature and geometric distortions, doppler smearing, and mechanism drift for the science spectra, and for temperature and geometric distortion, and mechanism drift for the wavecal spectra, were extracted using *Cedar*, each segment independently, using the default extraction paramenters used by CalCOS. The resulting 1d files contain then counts vs pixel.

The on-orbit separation, in pixels, between each segment of the PSA and WCA data, was determined by first cross-correlating the 1d WCA spectra with a PtNe line list, so that wavelengths can be assigned to each of the PtNe emission lines seen in pixel space. Each emission line, i, has then a pixel coordinate, $\mathrm{WCA_{SMOV,i}}$.

The heliocentric correction is only applied by the pipeline when wavelengths are being assigned. Since our analysis of the science data was done in pixel space, this correction was not applied. However, since for all the exposures analyzed here $|v_{\mathrm{Helio}}| \leq 2$ km/s this effect can be neglected as it is less than 0.5 pixels for both the M and L gratings.

The next step is to identify the pixel positions in the 1d PSA spectra, corresponding to the wavelengths of the PtNe emission lines, identified in the previous step, $\mathrm{PSA_{SMOV,i}}$. In the case of data obtained in Visits 50 and 73 for NGC 330–B37 this was accomplished by using the STIS/E140M spectrum of this target. For each feature corresponding to the wavelength being considered, the STIS spectrum was used as a guide, so that the pixel position of the same feature could be looked up in pixel space, in the 1d

PSA COS spectrum. For each grating/cenwave/segment, this procedure was applied to as many features as possible so that one can determine $PSA_{SMOV,i}$ - $WCA_{SMOV,i}$ across each segment of the FUV detector. The on-orbit separation between the PSA and WCA data is then calculated, for each grating/cenwave/segment, by calculating the mean of ($PSA_{SMOV,i}$ - $WCA_{SMOV,i}$) = PSA_{SMOV} - WCA_{SMOV}.

Table 2 summarizes the different measurements using data obtained in Visits 50 and 73 of program 11487. For each grating and cenwave, column 6 contains the mean of ($PSA_{SMOV,i}$ - $WCA_{SMOV,i}$), column 7 contains the separation between the TV03 and on-orbit lamp templates, WCA_{TV03} - WCA_{SMOV}, and column 8 contains PSA_{SMOV} - WCA_{SMOV} - (WCA_{TV03} - WCA_{SMOV}). Column 4 indicates which exposures were used to determine PSA_{SMOV} - WCA_{SMOV} and column 5 gives the number of features used to calculate the mean value given in column 6. For segment B of the G140L/1230 setting there is no lamp wavecal, and so the values quoted are those derived for segment A of the same setting.

3.2 NGC 6833

The analysis of NGC 6833 requires some care and will be done in the near future - since this is a slightly extended source the extraction of the 1d spectra has to be done in a special way to minimize the contamination of the emission profiles by the extended part of the nebula. This target is used as a confirmation of the wavelength scales, and not as a primary target, as there is no other independent source to confirm the wavelengths seen in the COS data (as done for NGC 330–B37 with STIS data). In addition, for emission lines produced by known species and for which the wavelengths can be calculated by taking the nebula radial velocity into account, there is still some uncertainty in those wavelengths, given that the emission lines are typically broad and their centroid can be influenced by how the 1d extraction was performed.

3.3 Wavelength Calibration in CalCOS

Program 11487 was executed during SMOV to obtain spectra of external targets, that would allow us to determine the on-orbit offsets between the PSA and WCA data, together with dataobtained in program 11488. These offsets are then used to place the dispersion relations derived in TV03 in the on-orbit frame of reference, so that correct wavelengths can be assigned to the on-orbit COS data, using the TV03-derived dispersion coefficients for the PSA.

Wavelength calibration by the COS pipeline is described in detail in the *COS Data Handbook* (Shaw et al. 2009); here we only present a summary.

The COS pipeline determines the dispersion-direction shift that needs to apply to the science data (PSA) to correct shifts due to the non-repeatability of the OSM mechanism by comparing the wavecal data (WCA) obtained concurrently (if in tagflash mode) with the data contained in the lamp template reference file. This reference file

contains one entry per FP-POS for each of the available modes, and so the wavecal data is compared with the lamp data at the same FP-POS. The lamp template reference file contains also a column that gives the separation in pixels between the lamp template at FP-POS = 3 and the lamp templates at the other FP-POS. The shift determined by comparing the wavecal data to the lamp plus the shift read from the column of the lamp template reference file are applied to the data, producing the $xfull$ pixel coordinate.

The COS pipeline computes then the wavelength from the $xfull$ pixel coordinate, as $xprime = xfull + d_{\rm PSA}$, where $d_{\rm PSA} = d_{\rm TV03} - d$. $d_{\rm TV03}$ is the separation between the PSA and WCA data in TV03, $\rm PSA_{TV03}$ - $\rm WCA_{TV03}$, and d is the separation between the PSA and WCA data on-orbit (SMOV), taking into account that the WCA data in SMOV is offset from the WCA in TV03: d = $\rm PSA_{SMOV}$ - $\rm WCA_{SMOV}$ - ($\rm WCA_{TV03}$ - $\rm WCA_{SMOV}$). The wavelengths are then computed from $\lambda = a_0 + a_1 \times xprime + a_2 \times xprime^2$, where a_0, a_1, and a_2 are the dispersion coefficients derived from TV03 data. Each segment of each grating/cenwave mode has its own dispersion solution. For the M gratings the a_2 term is zero.

4. Results

The offsets presented in column 7 of Table 2, d, were used to update the FUV wavelength dispersion reference file. This updated reference file was then used to process COS data obtained in three SMOV programs (independent from the programs used for wavelength calibration), so that the accuracy of the wavelength scales can be determined.

Table 3 presents the COS data from these three additional programs that was calibrated with the updated dispersion reference file, as well as existing STIS exposures that are used to evaluate the COS wavelength scales. All the COS data were processed through CalCOS (version 2.11f) and all the calibration switches were set to *PERFORM*, except for *TDSCORR*, *STATFLAG*, and *BRSTCORR*, which were set to *OMIT*. The STIS data were retrieved from the MAST archive. To facilitate the comparison between the COS and STIS wavelength scales, the STIS/E140H data used for comparison with the COS M resolution data and the STIS/E140M data used for comparison with the COS/G140L data, were convolved with the COS LSF appropriate to the COS grating being compared and appropriate to the wavelength in question (see Ghavamian et al. 2009).

Figure 1 compares wavelength calibrated COS G130M/1291 data for SK 155 (program 11489, FP-POS = 3; COS External Spectroscopic Performance - Part I) and STIS/E140H data for the same target (red). STIS data convolved with the LSFs appropriate to the wavelengths and settings displayed (see Ghavamian et al. 2009) are also shown (green). For segment A the COS and STIS wavelengths are in good agreement; for segment B the COS wavelengths are under-predicted by $\sim$4 pixels at 1190 Å while at 1260 Å they are under-predicted by $\sim$2 pixels.

Figure 2 also compares the wavelength scale of G130M/1291, but this time using a

different COS dataset. Two wavelength regions each, for segments A and B, from COS data of SK 191 (program 11997; COS Internal/External Wavelength Scale Monitor) are displayed in black, while red shows the STIS/E140M spectrum of the same target. For segment A the COS wavelengths are over-predicted by $\sim$1 pixel while for segment B the 1190 Å region is under-predicted by $\sim$1 pixel. The segment B COS wavelengths are in good agreement with the STIS wavelengths for the 1260 Å region.

Figure 3 compares the wavelength scales of G160M/1600, using COS data of SK 191 (same program as in Figure 2), with that of STIS E140M data, for segments A and B. For segment A there is good agreement between the COS and STIS wavelengths, while for segment B the COS wavelengths are under-predicted by $\sim$1 pixel.

Figure 4 compares wavelength calibrated COS G160M/1623 data for SK 155 (program 11489, COS External Spectroscopic Performance - Part I, all FP-POS combined) with that of STIS E140H for the same target (red). STIS data convolved with the LSF appropriate to the wavelengths and settings displayed are also shown (green). For segment A the COS wavelengths are over-predicted by $\sim$3 pixels, for segment B the COS wavelengths are in good agreement with those of STIS at $\sim$1526 Å, but they are under-predicted by $\sim$3 pixels at $\sim$1609 Å.

Figure 5 compares the wavelength scales of G140L/1230 and G140L/1105, using COS data of NGC 330–B37 (program 11487, COS FUV Internal/External Wavelength Scales, FP-POS=3), with that of STIS E140M (red), for two wavelength regions of segment A. STIS data convolved with the LSFs appropriate to the wavelengths and settings displayed are also shown (green). For G140L/1230 the COS wavelengths are over-predicted by $\sim$3 pixels for 1335 Å and under-predicted by $\sim$1 pixel for 1609 Å. For G140L/1105 the COS wavelengths are under-predicted by $\sim$2 pixels for 1335 Å and they agree well with those of STIS at 1609 Å.

Evaluating the COS FUV wavelength scales in the figures discussed above is made complicated by two issues that affect the COS FUV data. One of this issues is due to the wings of the LSF, which fill the cores of the saturated lines, affecting also the depths of weaker non-saturated lines (for more on the LSF see Ghavamian et al. 2009). We tried to minimize this effect by convolving the STIS E140H (SK 155) and E140M (NGC 330–B37) data with the COS LSFs. Note that no convolution was applied to the STIS data used for the comparisons presented in Figures 2 and 3, and so its possible that some of the discrepancies between the profiles are due to this. The other issue is related to the fact that currently no flat-fielding is applied to FUV data and as a result the shadows from the gain efficiency (GE) grid wires produce features that are similar to absorption lines and that change the profiles of real absorption lines.

Even though the figures discussed above seem to indicate that the accuracy of the wavelength scales is within the specifications defined in Table 4, the limited number of datasets on which the updated wavelength scales have been tested makes any conclusions preliminary. More work is required to further refine our evaluation of the FUV wavelength scales in the future. This is discussed below.

5. Reference Files Delivered

As a result of the work described in this ISR the reference files below were delivered to CDBS for use in COS on-the-fly reprocessing (OTFR) on January 29, 2010. Calibrated data obtained from the archive after this date will use these updated reference files (as long as the data were obtained after the USEAFTER date of each file). The files are: u1t1616nl_lamp.fits (FUV lamp template reference file; USEAFTER= 'August 17 2009 00:00:00') and u1t1616ml_disp.fits (FUV wavelength calibration reference file; USEAFTER= 'August 17 2009 00:00:00').

6. Future Work

- NGC 6833 data obtained in program 11487 will be analysed in the near future. Offsets between the PSA and WCA will be measured for this dataset and they will be compared to the offsets derived from the analysis of NGC 330–B37. Attempts will be made, whenever a reasonable number of emission lines is available, to determine the dispersion solutions directly from this dataset. These dispersion solutions will then be compared to the dispersion solutions derived from the TV03 data.
- Dispersion solutions will be derived for the WCA aperture, using the data obtained in program 11488; they will then be compared to the wavelength dispersion solutions derived in TV03 for this aperture, in order to determine if they are the same (minus a small offset in pixels).
- A Cycle 17 calibration program, 11997, is in place to monitor the stability of the PSA to WCA offsets on-orbit. This program observes Sk 191 (G130M cenwaves 1291 and1309; G160M cenwaves 1600 and 1623) and NGC 330–B37 (G140L cenwaves 1105 and 1230).
- GO and GTO datasets will be probed to search for datasets with a larger number of emission or absorption lines spread across the FUV detector that will permit an independent evaluation of the FUV wavelength scales.
- There will be a Cycle 17 Calibration program that will obtain data to improve the wavelength calibration of the segment B of the G140L/1230 setting (1280 in Cycle 18), which covers the wavelength region down to the Lyman limit.

7. Change History for COS ISR 2010-06

Version 1: 19 February 2010 - Original Document

References

Ghavamian, P., et al. 2009, COS Instrument Science Report 2009-01
Shaw, B. et al. 2009, "COS Data Handbook", Version 1.0, (Baltimore: STScI).

Table 1. Wavelength calibration exposures obtained in program 11487

Visit	Target	Grating	Cenwave	FP-POS
01	NGC 6833	G160M	1600	1,2,3,4
			1577	3
			1611	3
			1623	3
		G130M	1309	1,2,3,4[a]
			1291	3 [a]
			1300	3 [a]
			1318	3 [a]
			1327	3 [a]
		G140L	1230	3
50	NGC 330–B37	G160M	1600	1,3,4
		G130M	1309	1,3,4
		G140L	1230	3,4
73	NGC 330–B37	G160M	1600	3
		G130M	1309	3
			1291	3
			1300	3
			1318	3
			1327	3
		G160M	1577	3
			1589	3
			1611	3
			1623	3
		G140L	1230	1,2,3
			1105	3

[a]Segment A only.

Table 2. FUV offsets determined from program 11487

Grating	Cenwave	Segment	Exposure	# lines	$PSA_{SMOV} - WCA_{SMOV}$ (pix)	$WCA_{TV03} - WCA_{SMOV}$ (pix)	d (pix)
G130M	1291	FUVA	labp73giq	9	−43.9500	545.549	-589.499
		FUVB	labp73giq	6	−43.9100	539.081	-582.991
	1300	FUVA	labp73gkq	6	−45.1250	497.598	-542.723
		FUVB	labp73gkq	7	−43.1571	493.395	-536.552
	1309	FUVA	labp50alq, labp73gg	12	−43.1108	460.714	-503.8245
		FUVB	labp50alq, labp73gg	18	−42.9489	452.028	-494.977
	1318	FUVA	labp73gmq	5	−42.0080	480.279	-522.287
		FUVB	labp73gmq	8	−42.9312	467.639	-510.570
	1327	FUVA	labp73goq	5	−41.8940	449.035	-490.929
		FUVB	labp73goq	9	−43.9300	431.948	-475.878
G160M	1577	FUVA	labp73gqq	5	−44.1720	-4.49852	-39.673
		FUVB	labp73gqq	5	−43.1140	-4.19682	-38.917
	1589	FUVA	labp73gsq	6	−43.7133	-21.8603	-21.853
		FUVB	labp73gsq	4	−41.4575	-23.1098	-18.348
	1600	FUVA	labp73geq	5	−41.8280	-27.4868	-14.341
		FUVB	labp73geq	9	−40.8389	-31.9993	-8.840
	1611	FUVA	labp73guq	10	−45.4032	-44.3193	-1.084
		FUVB	labp73guq	13	−43.6799	-53.2402	9.560
	1623	FUVA	labp73gwq	12	−45.4716	-48.4831	3.012
		FUVB	labp73gwq	18	−43.5691	-63.0932	19.524
G140L	1105	FUVA	labp73hhq	13	−44.4749	-42.3273	-2.148
	1230 [a]	FUVA	labp50arq, labp73h8q	16	−45.8595	-66.0997	20.240
		FUVB	-		−45.8595	-66.0997	20.240

[a]G140L/1230 for Cycle 17 will become G140L/1280 for Cycle 18 and new offsets will be determined for this new cenwave.

Note. — Exposures labp50* and labp73* are from visits 50 and 73, respectively, of program 11487, which observed NGC 330–B37. Column 5 contains the number of points used to calculate the entries in Column 6, which contains the on-orbit separation between PSA and WCA data, PSA_{SMOV} - WCA_{SMOV} = mean ($PSA_{SMOV,i}$ - $WCA_{SMOV,i}$); column 7 contains the separation between the TV03 and on-orbit lamp templates WCA_{TV03} - WCA_{SMOV}; the last column contains d, the difference between columns 5 and 6, PSA_{SMOV} - WCA_{SMOV} - (WCA_{TV03} - WCA_{SMOV}).The offsets for segment B of G140L/1230 are assumed to be the same as those for G140L/1230/FUVA, since the PtNe lamp does not produce counts at these short wavelengths.

Table 3. COS and STIS data used to compare FUV wavelength scales

Target	Grating/Cenwave	Aperture	Exposure	Time (sec)	Program
SK 191/COS	G130M/1291/FP=3	PSA	lbby0104q	88	11997
SK 191/COS	G160M/1600/FP=3	PSA	lbby01uaq	120	11997
SK 191/STIS	E140M	0.2x0.2	o6df03030	3236	9116
SK 155/COS	G130M/1291/FP=3	PSA	laaf1aixq		11489
SK 155/STIS	E140H	0.2x0.09	o5dw01010	2305	8145
SK 155/COS	G160M/1623/FP=all	PSA	laaf1a0b0	640	11489
SK 155/STIS	E140H	0.2x0.09	obcd01010	2150	12010
	E140H	0.2x0.09	obcd01020	3150	12010
NGC 330–B37/COS	G140L/1230/FP=3	PSA	labp73gyq	360	11487
	G140L/1105/FP=3	PSA	labp73hhq	360	11487
NGC 330–B37/STIS	E140M	0.2x0.2	o6df20020	2259	9116
	E140M	0.2x0.2	o6df20030	3236	9116
	E140M	0.2x0.2	o6df21020	2259	9116
	E140M	0.2x0.2	o6df21030	3236	9116

Note. — STIS exposures obcd01010 and obcd01020 (used for comparison with SK 155/COS/G160M) were coadded to increase the S/N of the resulting dataset. All the STIS exposures for NGC 330–B37 were also coadded to increase the S/N of the resulting dataset.

Table 4. COS Specifications for FUV Wavelength Accuracies

Grating	Error Goal (1σ) (km s^{-1})	Error Goal (1σ) (pixels)	Internal Error (pixels)
G130M	15	5.7–7.5	3.0–4.0
G160M	15	5.8–7.2	3.1–3.8
G140L	150	7.5–12.5	4.0–6.6

Note. — The internal error includes the accuraccy of the wavelength scale, the dispersion relation, aperture offsets, distortions and drifts. The error goal includes contributions from external sources, which are dominated by target mis-centering in the aperture. Error goal given per exposure.

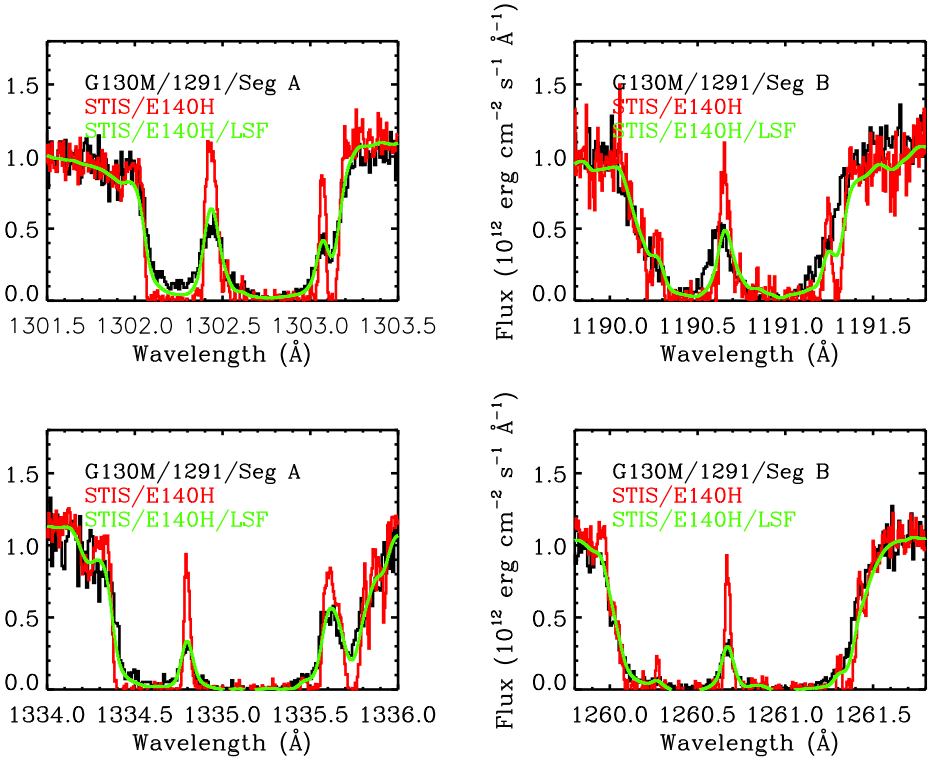

Figure 1. Comparison between wavelength calibrated COS G130M/1291 data for SK 155 (black) and STIS/E140H data for the same target (red). STIS data convolved with the LSF appropriate to the wavelengths and settings displayed are also shown (green). For segment A the COS and STIS wavelengths are in good agreement; for segment B the COS wavelengths are under-predicted by ∼4 pixels at 1190 Å while at 1260 Å they are under-predicted by ∼2 pixels. COS data is from program 11489, for FP-POS = 3.

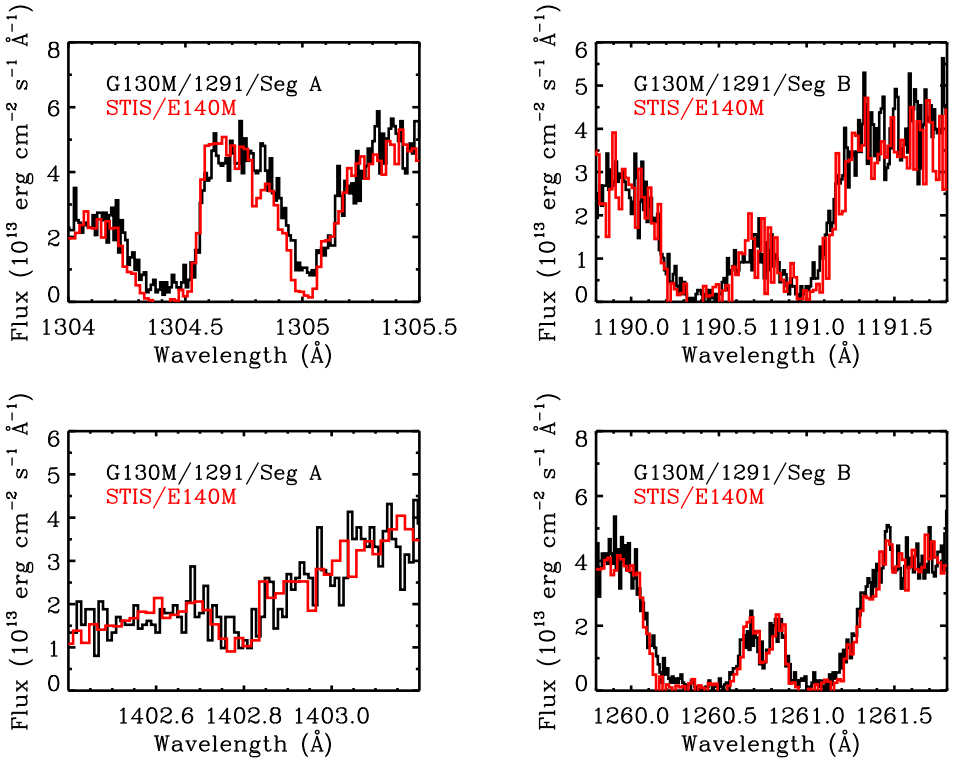

Figure 2. Comparison between STIS/E140M (red) and COS/G130M/1291 (black) wavelength scales using SK 191 data. COS data is from program 11997, for FP-POS = 3.

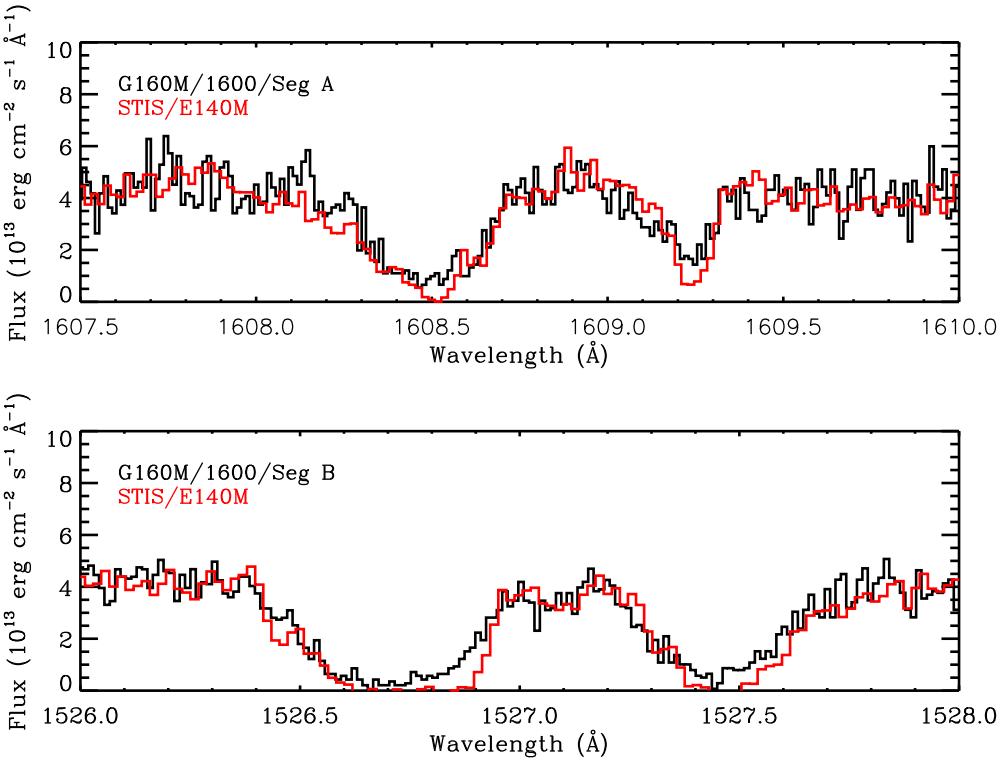

Figure 3. Comparison between STIS/E140M (red) and COS/G160M/1600 (black) wavelength scales using SK 191 data. COS data is from program 11997, FP-POS = 3

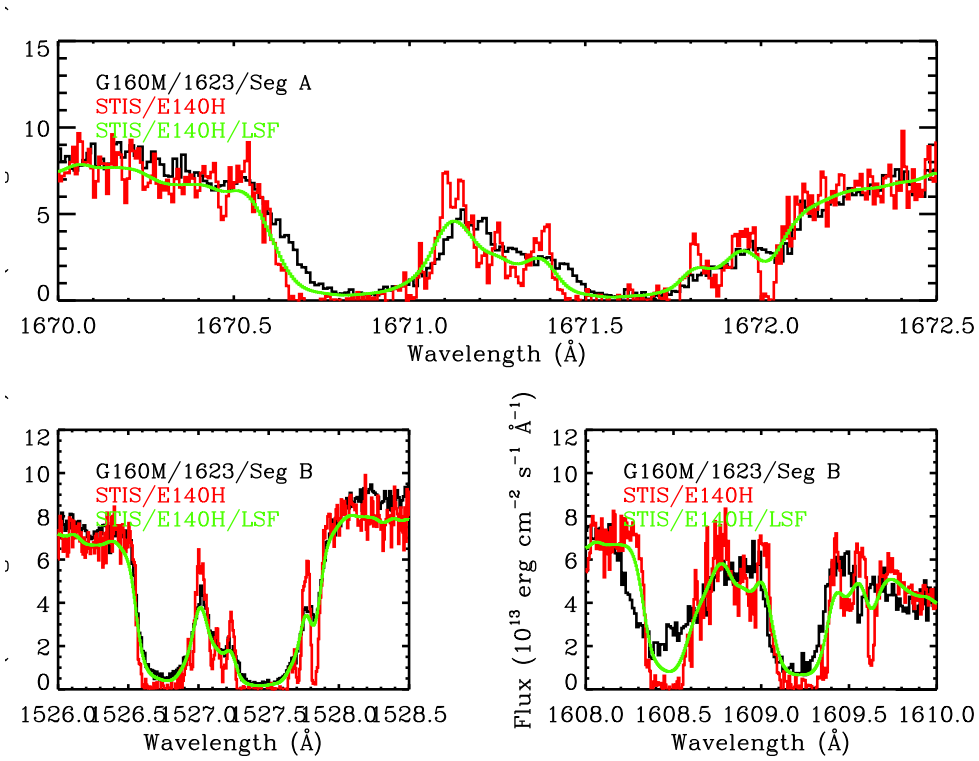

Figure 4. Comparison between wavelength calibrated COS G160M/1623 data for Sk 155 (black) and STIS/E140H data for the same target (red). STIS data convolved with the LSF appropriate to the wavelengths and settings displayed are also shown (green). For segment A the COS wavelengths are over-predicted by ∼3 pixels; for segment B the 1526 Å wavelength region the COS wavelengths are in good agreement with those from STIS, while at 1609 Å they are under-predicted by ∼3 pix. COS data is from program 11489, FP-POS = 1,2,3,4 (combined).

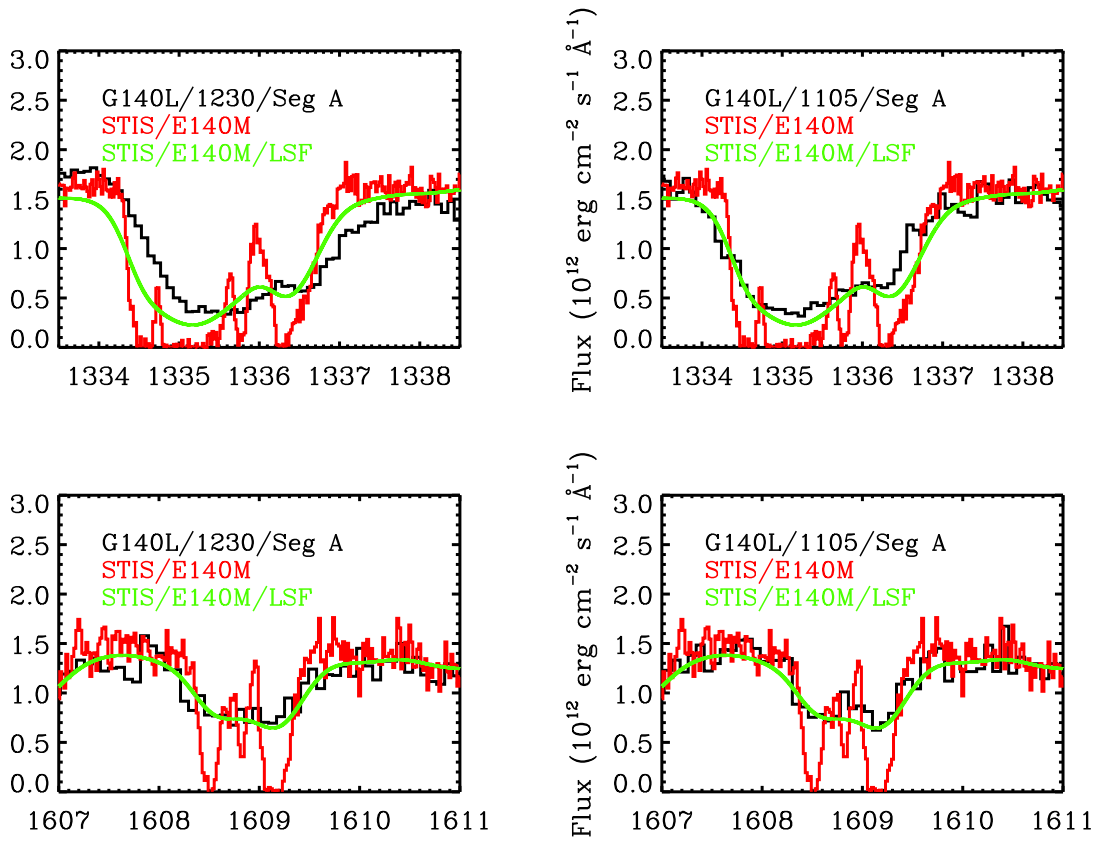

Figure 5. Comparison between wavelength calibrated COS G140L/1230 (left panel) and G140L/1105 (right panel) fo NGC 330–B37 (black) and STIS E140M data for the same target (red). STIS data convolved with the LSF appropriate to the wavelengths and settings displayed are also shown (green). For G140L/1230 the COS wavelengths are over-predicted by ∼3 pixels for 1335 Å and under-predicted by ∼1 pixel for 1609 Å. For G140L/1105 the COS wavelengths are under-predicted by ∼2 pixels for the 1335 Å region and they agree well with those of STIS at 1609 Å. COS data is from program 11487, for FP-POS = 3 (these exposures were not used to derive the offsets).